Journal of
Applied Crystallography
ISSN 0021-8898
Editor: **Gernot Kostorz**

A new approach to wide-angle dynamical X-ray diffraction by deformed crystals

S. G. Podorov, N. N. Faleev, K. M. Pavlov, D. M. Paganin, S. A. Stepanov and E. Förster

Journal of
Applied Crystallography
ISSN 0021-8898

Received 4 May 2006
Accepted 4 July 2006

A new approach to wide-angle dynamical X-ray diffraction by deformed crystals

S. G. Podorov,[a]* N. N. Faleev,[b] K. M. Pavlov,[a,c] D. M. Paganin,[a] S. A. Stepanov[d] and E. Förster[e]

[a]School of Physics, Monash University, Victoria 3800, Australia, [b]ECE Department, University of Delaware, Newark, DE 19716, USA, [c]Monash Centre for Synchrotron Science, Monash University, Victoria 3800, Australia, [d]Argonne National Laboratory, 9700 South Cass Ave., Argonne, IL 60439, USA, and [e]Institute of Optics and Quantum Electronics, Friedrich-Schiller University, Jena, Germany. Correspondence e-mail: sergey.podorov@sci.monash.edu.au

A new approach is proposed for X-ray dynamical diffraction theory in distorted crystals. The theory allows one to perform dynamical diffraction simulations between Bragg peaks for non-ideal crystals, using a simple approach of two distorted waves. It can be directly applied for reciprocal-space simulation. The formalism is used to analyse high-resolution X-ray diffraction data, obtained for an InSb/InGaSb/InSb/InAs superlattice grown on top of a GaSb buffer layer on a (001) GaSb substrate.

1. Introduction

High-resolution X-ray diffraction (see *e.g.* Fewster, 2003; Pietsch *et al.*, 2004) has become a standard tool for the non-destructive characterization of epitaxic layers, films and complex multilayer semiconductor structures, *e.g.* superlattices (SLs). The layer thickness, chemical composition and strain distribution within such multilayer structures can be successfully obtained by comparing experimental data with simulations, using well developed approaches to X-ray dynamical diffraction theory in deformed crystals (see *e.g.* Takagi, 1962; Taupin, 1964; Afanas'ev & Kohn, 1971; Pinsker, 1978; Bartels *et al.*, 1986; Härtwig, 2001). However, those approaches are restricted by the strong approximation of small angular deviation from the appropriate angular Bragg position θ_B ($|\theta - \theta_B| \ll 1$). Such an approximation results in incorrect angular peak positions for strongly strained layers in heterostructures or SLs (Zaus *et al.*, 1991; Servidori *et al.*, 1992).

To solve this problem, Zaus (1993) represented an inhomogeneous layer by a combination of thin homogeneous lamellae; for each lamella, he employed the dynamical diffraction theory for an ideal crystal. Such an approach can partially solve the problem; however, it does not take into account that the two-beam approximation will be incorrect for large deviation angles. Grundmann & Krost (2000) have tested all commercially available simulation programs, based on the dynamical diffraction theory, and found that these programs produce incorrect results for large angular scans. One of the major reasons, as they pointed out, is the two-beam diffraction restriction, where the appropriate simulation parameters are developed around only one vector in reciprocal space. The other reason, as they mentioned, lies in the approximations for the angular parameters $(k_h^2 - k_0^2)/k_0^2$ usually used in dynamical diffraction theories.

Grundmann & Krost (2000) have also reported that the generalized dynamical diffraction approach (De Caro *et al.*, 1997), taking into account *e.g.* all four solutions of the secular equation as well as the asymptotic sphericity of the dispersion surface, does not correctly describe the scattering intensity far from the appropriate Bragg position, again due to the two-beam diffraction approximation. As an alternative, they used kinematical diffraction theory. However, even for thin layers, the kinematical theory can produce incorrect results, *e.g.* in the case of multilayer structures, where the dynamical interaction between waves needs to be taken into account (Bartels *et al.*, 1986; Vardanyan *et al.*, 1985). Caticha (1994) used the Darwin (1914) approach for the case of symmetrical diffraction at an ideal (undeformed) crystal to build an extended version of the dynamical diffraction theory, which takes into account multiple beam effects within the two-beam formalism. However, he did not consider the important case of chemically inhomogeneous structures with an arbitrary deformation field, which is typical for modern opto- and microelectronic structures (see *e.g.* Fewster, 2003). Recently, Holý & Fewster (2003), using Laue-type theory and the 6×6 matrix formalism investigated the three-beam diffraction case in a crystal with a SL, which is an extension of the standard two-beam diffraction approach.

In this article, we introduce a new approach to X-ray dynamical diffraction theory in distorted crystals, which implicitly includes coplanar multiple beam diffraction in the two-beam diffraction case. It allows us to perform dynamical diffraction simulations between Bragg peaks for non-ideal crystals, using a simple approach of two distorted waves. We exclude from our consideration the limit cases (rarely used for multilayer structure characterization) of grazing incidence diffraction (see *e.g.* Stepanov *et al.*, 1998, and references therein) and when the Bragg angle is close to $\pi/2$ (see *e.g.*

Souvorov *et al.*, 2004, and references therein). We also do not consider the complex case of multiple beam diffraction when several strong reflections occur simultaneously (see *e.g.* Kohn, 1991; Okitsu, 2003, and references therein), because such a situation is usually avoidable by appropriate experimental planning. Further, we introduce a new integral representation for the angular shift caused by lattice deformations, which can also be employed for the case of relatively strong deformations causing interbranch scattering (Penning, 1966; Authier, 1967, 2005).

2. Theory

To describe dynamical X-ray diffraction by solving the Maxwell equations in a distorted crystal, the total wavefield will be sought as a composition of incident and diffracted waves:

$$\mathbf{E}(\mathbf{r}, \mathbf{s}) = \mathbf{E}_0(\mathbf{r}, \mathbf{s}) \exp(i\mathbf{k}_0\mathbf{r}) + \mathbf{E}_s(\mathbf{r}, \mathbf{s}) \exp(i\mathbf{k}_s\mathbf{r}). \quad (1)$$

Here, $|\mathbf{k}_0| = |\mathbf{k}_s| = k = 2\pi/\lambda$, λ is the wavelength in vacuum and $\mathbf{E}_{0,s}(\mathbf{r})$ are slowly varying functions for the transmitted and scattered wave, respectively. The vectors $\mathbf{k}_0$ and $\mathbf{k}_s$ are wavevectors of the incident and scattered waves, respectively, and $\mathbf{s} = \mathbf{k}_s - \mathbf{k}_0$ are the scattering vectors. Note that the effects of refraction, attenuation and dispersion in the medium are represented in our approach through the slowly changing amplitudes $\mathbf{E}_{0,s}(\mathbf{r})$, in contrast to the usual dynamical diffraction approaches (see *e.g.* Pinsker, 1978; Authier, 2005) employing dispersion in the wavevectors $\mathbf{k}_{0,s}$.

From the Helmholtz equation (see *e.g.* Afanas'ev & Kohn, 1971),

$$\Delta\mathbf{E}(r) + k^2[1 + \chi(r)]\mathbf{E}(r) = 0, \quad (2)$$

we obtain (see also Podorov & Förster, 2000)

$$\left[2i(\mathbf{k}_0 \cdot \nabla)\mathbf{E}_0 + k^2\chi(\mathbf{r})\mathbf{E}_0\right] \exp(i\mathbf{k}_0\mathbf{r}) + \left[2i(\mathbf{k}_s \cdot \nabla)\mathbf{E}_s + k^2\chi(\mathbf{r})\mathbf{E}_s\right] \exp(i\mathbf{k}_s\mathbf{r}) = 0, \quad (2a)$$

where χ is the polarizability of the crystal. If the deformation $\mathbf{u}(\mathbf{r})$ does not cause the overlapping of the core electron wavefunctions of the displaced atoms (*i.e.* $\partial u_i/\partial x_j \ll 1$), the Takagi approximation (Takagi, 1962, 1969) $\chi(\mathbf{r}) = \chi^{\rm id}(\mathbf{r} - \mathbf{u}(\mathbf{r}))$ can be used (Kuriyama, 1967). Then the polarizability can be represented as (see *e.g.* Takagi, 1969)

$$\chi(\mathbf{r}) = \sum_g \chi_g(\mathbf{r}) \exp[i\mathbf{g}\mathbf{r} - i\mathbf{g}\mathbf{u}(\mathbf{r})]. \quad (3)$$

Here, $\mathbf{g}$ are reciprocal lattice vectors, and $\mathbf{u}(\mathbf{r})$ is the displacement of atoms from their positions in an ideal crystal lattice. We slightly modify the expression for the argument of the exponents in equation (3):

$$\begin{aligned}\mathbf{g}\mathbf{r} - \mathbf{g}\mathbf{u}(\mathbf{r}) &= \mathbf{g}\mathbf{r} - \int_0^{\mathbf{r}} \nabla[\mathbf{g}\mathbf{u}(\tilde{\mathbf{r}})]\, {\rm d}\tilde{\mathbf{r}} \\ &= \int_0^{\mathbf{r}} \left\{\mathbf{g} - \nabla[\mathbf{g}\mathbf{u}(\tilde{\mathbf{r}})]\right\} {\rm d}\tilde{\mathbf{r}} \\ &= \int_0^{\mathbf{r}} \tilde{\mathbf{g}}(\tilde{\mathbf{r}})\, {\rm d}\tilde{\mathbf{r}} \\ &= \int_0^{\mathbf{r}} \left[\frac{2\pi}{d(\tilde{\mathbf{r}})}\mathbf{n}_{\tilde{\mathbf{g}}}(\tilde{\mathbf{r}})\right] {\rm d}\tilde{\mathbf{r}}. \end{aligned} \quad (4)$$

Here $\tilde{\mathbf{g}}(\mathbf{r})$ is the local vector of the reciprocal lattice, $\mathbf{n}_{\tilde{\mathbf{g}}}$ is the local unit vector parallel to the vector $\tilde{\mathbf{g}}(\mathbf{r})$, and $d(\mathbf{r})$ is the local interplanar spacing. We also used the fact that $\mathbf{u}(0) \equiv 0$, where the origin corresponds to the surface of the crystal. Thus, by using equations (3) and (4), we do not need any higher-order correction for the deformation field [*e.g.* the second-order approximations used by De Caro *et al.* (1996) to describe the case of strong deformations], because our derivations use only the local interplanar spacings.

To divide equation (2*a*) into two independent differential equations, we multiply equation (2*a*) by the factor $\exp(-i\,\mathbf{k}_0\mathbf{r})$ and average over one elementary cell volume (see *e.g.* Takagi, 1962, 1969):

$$2i(\mathbf{k}_0 \cdot \nabla)E_0 + k^2E_0 \sum_{\mathbf{g}} \chi_{\rm g}(\mathbf{r})\alpha(\tilde{\mathbf{g}}, \mathbf{r}) + 2iC\beta(\mathbf{s})(\mathbf{k}_{\rm s} \cdot \nabla)E_{\rm s} + k^2CE_{\rm s} \sum_{\mathbf{g}} \chi_{\rm g}(\mathbf{r})\alpha(\tilde{\mathbf{g}} + \mathbf{s}, \mathbf{r}) = 0. \quad (5)$$

The same procedure with multiplicative factor $\exp(-i\,\mathbf{k}_{\rm s}\mathbf{r})$ gives

$$2i(\mathbf{k}_{\rm s} \cdot \nabla)E_{\rm s} + k^2E_{\rm s} \sum_{\mathbf{g}} \chi_{\rm g}(\mathbf{r})\alpha(\tilde{\mathbf{g}}, \mathbf{r}) + 2iC\beta(-\mathbf{s})(\mathbf{k}_0 \cdot \nabla)E_0 + k^2CE_0 \sum_{\mathbf{g}} \chi_{\rm g}(\mathbf{r})\alpha(\tilde{\mathbf{g}} - \mathbf{s}, \mathbf{r}) = 0, \quad (6)$$

$$\alpha(\mathbf{s} + \tilde{\mathbf{g}}, \mathbf{r}) = \frac{1}{V_{\rm e.c.}} \int_{V_{\rm e.c.}} \exp\left\{i \int_0^{\mathbf{r}} [\mathbf{s} + \tilde{\mathbf{g}}(\tilde{\mathbf{r}})]\, {\rm d}\tilde{\mathbf{r}}\right\} {\rm d}V, \quad (7)$$

$$\beta(\mathbf{s}) = \frac{1}{V_{\rm e.c.}} \int_{V_{\rm e.c.}} \exp(i\mathbf{s}\mathbf{r})\, {\rm d}V, \quad (8)$$

and $V_{\rm e.c.}$ is the volume of the elementary cell at point $\mathbf{r}$. C is the polarization factor, which is 1 for σ polarization and $(\mathbf{k}_0 \cdot \mathbf{k}_{\rm s})/k^2$ for π polarization. Note that in equations (5) and (6) we include the full range of Fourier components of the polarizability $\chi_{\rm g}$. This takes into account multiwave diffraction in a manner similar to that used by Caticha (1994). The factor $\alpha(\mathbf{s} - \tilde{\mathbf{g}}, \mathbf{r})$ includes the usual component $\exp\{i[\mathbf{s}\mathbf{r} - \mathbf{g}\mathbf{r} + \mathbf{g}\mathbf{u}(\mathbf{r})]\}$, and a small correction. Note that with correction [equation (4)] we fulfil the Bragg condition exactly. For the special case $\mathbf{s} \simeq \mathbf{g}$, equations (5) and (6) reduce to the Takagi–Taupin equations. The system of equations (5) and (6) extends the Takagi–Taupin theory for simulation of the reflection curve over very large angular ranges including several orders of reflection. As we use an arbitrary scattering vector, the theory is suitable for simulation of the reciprocal-space map of nano-sized structures.

As one of the applications of the theory, we consider a one-dimensional case where the functions $\mathbf{u}(\mathbf{r})$ and $\chi_g(\mathbf{r})$ depend only on the coordinate z. This approximation is applicable to a broad class of multilayer structures in which the layers are homogeneous in both lateral directions. We also restrict ourselves to modelling ω–2θ scans (rotation speed of the detector/analyser crystal is twice that of the sample) in the symmetrical geometry. Then $\mathbf{s} = s\mathbf{n} = 2k \sin\theta\, \mathbf{n}$, where θ is the angle between $\mathbf{k}_0$ and the crystal surface, and $\mathbf{n}$ is the outward normal to the crystal surface. Then the system of equations (5) and (6) can be transformed to a one-dimensional differential equation similar to the Taupin (1964) equation.

3. Application

We demonstrate the power of the new approach by studying, *via* high-resolution X-ray diffraction, an InSb/InGaSb/InSb/InAs superlattice grown on top of a GaSb buffer layer on a (001) GaSb substrate. This multilayered periodic hetero-composition was grown by molecular beam epitaxy (MBE) on a precisely oriented GaSb(001) substrate at ~773 K. A thick GaSb buffer layer (~0.5 μm) was used to improve the quality of the growth surface. The primary part of the periodical structure consisted of one monolayer of InSb, 4.5 nm of $Ga_xIn_{1-x}Sb$, one monolayer of InSb and 9 nm of InAs, repeated 60 times to form a superlattice. The composition of the $Ga_xIn_{1-x}Sb$ layers perfectly matched the average lattice parameter of the periodic structure to the lattice parameter of the GaSb substrate.

X-ray measurements were performed on a Rigaku Ultima III X-ray diffractometer aligned to quasi-high-resolution mode with a high-brilliance multilayer mirror, two-bounce Ge(110) monochromator, 220 reflection, and narrow receiving slits in front of the detector. Corresponding ω–2θ rocking curves (RCs) were measured over a wide angular range, including diffracted RCs around the GaSb 002, 004 and 006 reflections. Extensive interference patterns revealed high crystalline perfection of the investigated structure: indeed, the estimated roughness of the interfaces is less than a couple of monolayers. We did not observe any overlapping or non-coincidence of SL peaks from different reflections, caused by unevenness of the period of the SL in comparison with the main lattice parameter (Schuster *et al.*, 1995). The SL peaks smoothly turn from one reflection into the other, without visible interruptions.

The extended diffraction pattern, measured around the GaSb 004 reflection, is shown in Fig. 1. Along with the main superlattice peaks, corresponding to the main superlattice period of the heterostructure (14.5 nm), all RCs show additional sharp peaks between major satellites, equidistant from the main SL peaks and corresponding to an additional super-superlattice periodicity (Punegov, 2003; Rettig *et al.*, 1998), unintentionally created during epitaxic growth, probably as a result of a small periodic change of the In incorporation rate at epitaxic layers.

Equations (5) and (6) were solved numerically by a fourth-order Runge–Kutta method in the one-dimensional case, and were subsequently used for curve fitting. Preliminary calculations and best fits have shown that the period of the super-superlattice variations is about 2.5 times greater than the period of the main superlattice. It was deduced that the main superlattice period is equal to 14.5 nm and the additional super-superlattice period is equal to 36.0 nm (see Fig. 2 and Table 1). As the present theory is not formulated in terms of the deformation field, but rather in terms of the lattice parameter distribution $a(z)$, it could give a means to determine the lattice-parameter distribution with greater precision. It is

Table 1
Best-fit parameters for an InSb/InGaSb/InSb/InAs superlattice.

Layers 1 through 4 are repeated 60 times to form the superlattice.

Layer	Chemical composition	Thickness	Average interplanar spacing for 004 reflection plane
1	InSb	0.7 nm	0.1575 nm†
2	$Ga_xIn_{1-x}Sb$	4.3 nm	0.1530 nm†
3	InSb	0.7 nm	0.1575 nm†
4	InAs	8.8 nm	0.1515 nm
5	GaSb	(001)-GaSb substrate	0.1524 nm

† These parameters vary with a superperiod of 36.0 nm and modulation amplitude of 0.0004 nm; see Fig. 2.

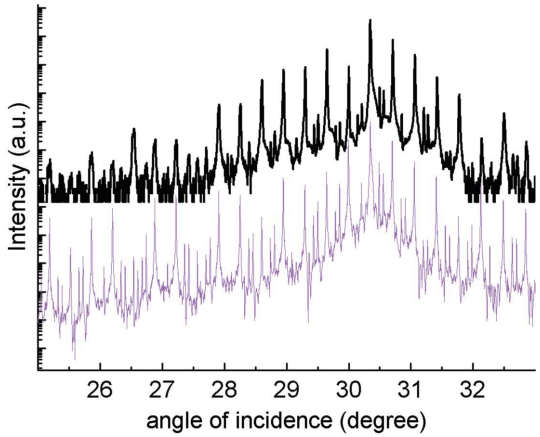

Figure 1
Experimental rocking curve (upper) for GaSb 004 reflection and fitted simulated curve. Intensity is shown on logarithmic scale; curves are displaced vertically for clarity.

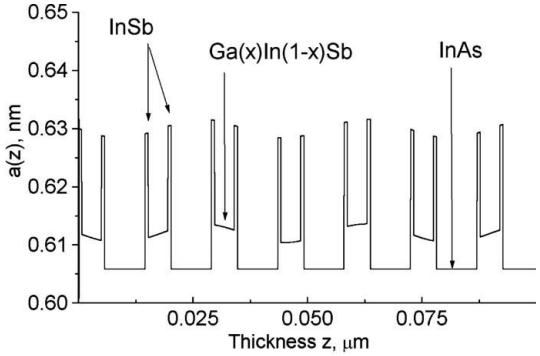

Figure 2
Lattice parameter in the InSb/InGaSb/InSb/InAs superlattice (fragment).

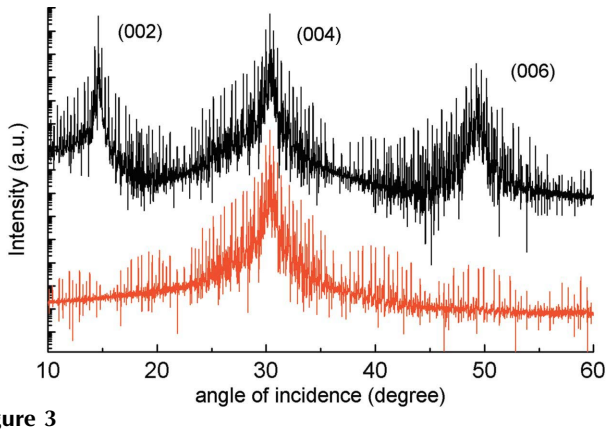

Figure 3
Simulated curves from present theory (upper) and from Takagi–Taupin theory with Zaus correction. Intensity is shown on logarithmic scale; curves are offset for clarity.

possible to conclude from our simulations that within the SL period, two InSb monolayers, divided by the GaInSb layer, have different interplanar spacing and hence slightly different chemical composition due to layer intermixing. Small differences between the simulated and the experimental rocking curves may be explained by an additional weak variation of chemical composition in the multilayers. A difference between our method and the conventional Takagi–Taupin theory with Zaus correction of the angular variable (Zaus, 1993) is shown in Fig. 3. The present theory gives a simple way to simulate reflection curves over a very large angular range. For simulation of diffraction by crystals with three-dimensional deformation fields, see the work of Podorov & Förster (2000).

4. Conclusion

In summary, we have introduced a new approach to X-ray dynamical diffraction theory in distorted crystals. The theory allowed us, for the first time, to perform multiwave dynamical diffraction simulations between Bragg peaks for non-ideal crystals, using a simple approach of two distorted waves. The formalism was then applied to yield precise structural information for an InSb/InGaSb/InSb/InAs superlattice, from high-resolution X-ray diffraction data. We anticipate that the new formalism may sharpen the precision with which X-ray diffraction is employed as an analytical tool for the non-destructive quantitative characterization of epitaxic layers, films and complex multilayer semiconductor structures.

The authors acknowledge funding from the Australian Research Council.

References

Afanas'ev, A. M. & Kohn, V. G. (1971). *Acta Cryst.* A**27**, 421–430.
Authier, A. (1967). *Adv. X-ray Anal.* **10**, 9–31.
Authier, A. (2005). *Dynamical Theory of X-ray Diffraction*, revised ed. Oxford University Press.
Bartels, W. J., Hornstra, J. & Lobeek, D. J. W. (1986). *Acta Cryst.* A**42**, 539–545.
Caticha, A. (1994). *Phys. Rev. B*, **49**, 33–38.
Darwin, C. G. (1914). *Philos. Mag.* **27**, 315, 675.
De Caro, L., Giannini, C. & Tapfer, L. (1996). *J. Appl. Phys.* **79**, 4101–4110.
De Caro, L., Giannini, C. & Tapfer, L. (1997). *Phys. Rev. B*, **56**, 9744–9752.
Fewster, P. F. (2003). *X-ray Scattering from Semiconductors*, 2nd ed. London: Imperial College Press.
Grundmann, M. & Krost, A. (2000). *Phys. Status Solidi. B*, **218**, 417–423.
Härtwig, J. (2001). *J. Phys. D Appl. Phys.* **34**, A70–A77.
Holý, V. & Fewster, P. F. (2003). *J. Phys. D Appl. Phys.* **36**, A5–A8.
Kohn, V. G. (1991). *J. Mosc. Phys. Soc.* **1**, 425–434.
Kuriyama, M. (1967). *J. Phys. Soc. Jpn*, **23**, 1369–1379.
Okitsu, K. (2003). *Acta Cryst.* A**59**, 235–244.
Penning, P. (1966). PhD thesis, Technical University of Delft, The Netherlands.
Pietsch, U., Holý, V. & Baumbach, T. (2004). *High Resolution X-ray Scattering: from Thin Films to Lateral Nanostructures*, 2nd ed. New York: Springer-Verlag.
Pinsker, Z. G. (1978). *Dynamical Scattering of X-rays in Crystals*. Heidelberg: Springer.
Podorov, S. G. & Förster, E. (2000). *Phys. Status Solidi B*, **220**, 829–836.
Punegov, V. I. (2003). *Tech. Phys. Lett.* **29**, 815–818.
Rettig, R., Marschner, T., Stolz, W. & Tapfer, L. (1998). *J. Appl. Phys.* **84**, 237–247.
Schuster, M., Lessmann, A., Munlholm, A., Brennan, S., Materlik, G. & Riechert, H. (1995). *J. Phys. D Appl. Phys.* **28**, A206–A211.
Servidori, M., Cemballi, F., Fabbri, R. & Zani, A. (1992). *J. Appl. Cryst.* **25**, 46–51.
Souvorov, A., Ishikawa, T., Nikulin, A. Y., Stetsko, Y. P., Chang, S. L. & Zaumseil, P. (2004). *Phys. Rev. B*, **70**, 224109.
Stepanov, S. A., Kondrashkina, E. A., Köhler, R., Novikov, D. V., Materlik, G. & Durbin, S. M. (1998). *Phys. Rev. B*, **57**, 4829–4841.
Takagi, S. (1962). *Acta Cryst.* **15**, 1311–1312.
Takagi, S. (1969). *J. Phys. Soc. Jpn*, **26**, 1239–1253.
Taupin, D. (1964). *Bull. Soc. Fr. Miner. Crist.* **87**, 469–511.
Vardanyan, D. M., Manoukyan, H. M. & Petrosyan, H. M. (1985). *Acta Cryst.* A**41**, 212–217.
Zaus, R. (1993). *J. Appl. Cryst.* **26**, 801–811.
Zaus, R., Schuster, M., Göbel, H. & Reithmaier, J. P. (1991). *Appl. Surf. Sci.* **50**, 92–96.